Eur. Phys. J. A **24**, 137–147 (2005)
DOI 10.1140/epja/i2004-10127-4

THE EUROPEAN PHYSICAL JOURNAL A

Elastic scattering via quark structure of nucleons

M.M.H. El-Gogary, A.Y. Ellithi[a], M.Kh. Hegab, and A.A. Mohamed

Physics Department, Faculty of Science, Cairo University, Giza, Egypt

Received: 21 July 2004 / Revised version: 7 September 2004 /
Published online: 25 February 2005 –
Communicated by V. Vento

Abstract. In the framework of the Glauber multiple-scattering theory, the elastic collisions of proton-proton (pp) at the center-of-mass energies $\sqrt{s} = 23.5$, 30.7, 44.7, and 52.8 GeV and alpha-proton (αp) at $\sqrt{s} = 88$ and 89 GeV are analyzed by considering the quark structure of their constituents. The differential cross-section containing the full multiple-scattering series between their quarks is calculated using Gaussian forms for the quark density and quark-quark (QQ) scattering amplitudes. The results obtained from the quark model and the conventional nucleon model are compared with the experimental data. The comparison shows that the nucleon model reproduces the experimental data more satisfactorily than the quark model, and both approaches have limited success in describing the data at such energies. The agreement with the experimental data is improved by the inclusion of the phase variation.

PACS. 25.40.Cm Elastic proton scattering – 25.45.De Elastic and inelastic scattering – 25.60.Bx Elastic scattering – 24.85.+p Quarks, gluons, and QCD in nuclei and nuclear processes

1 Introduction

Over many years, the scattering of high-energy composite particles has been a powerful tool for probing the structure of their constituents and studying the scattering mechanisms. Experiments of such interactions have shown that the differential cross-sections exhibit the effects to various degrees of multiple scattering depending on the incident energy and the mass number of the interacting composite systems [1]. In particular, the diffraction pattern appears at small scattering angles (small momentum transfers (q)), while at large angles the cross-section values decay many orders of magnitude smaller than those in the forward direction [2–4]. However, accumulation of data with such details is useful to test and improve the theoretical models concerned. The multiple-scattering theory of Glauber [5] is one of the suitable approaches to describe such collisions. The theory is based on high-energy approximation, in which the interacting particles are almost frozen in their instantaneous positions during the passage of the projectile through the target. With this approximation, the scattering amplitudes of the composite particles are simply expressed in terms of a multiple-scattering series based on the *free* two-particle collision. As a matter of fact, these calculations have shown disagreements with the experimental data even at forward angles [6] and/or unphysical divergence at large momentum transfers [7–9]. These earlier calculations have been utilized with further approximations. In particular, the multiple-scattering series is truncated to low orders of scattering and the effect of the center-of-mass correlation is treated as a global correction multiplied by the scattering amplitude. The calculations [7–9] up to the fourth order of the multiple-scattering series are shown to be necessary to enhance the predictions at large angles [8].

Also, the large q-divergence is removed by incorporating the center-of-mass correlations in the phase shift function in each order of the scattering term [7,9]. The full Glauber multiple-scattering series calculation is computationally difficult for collision of two composite systems of mass numbers $A, B > 4$ [10]. In fact, the series describing these collisions contains numerous $(2^{A\times B} - 1)$ terms so that its complete summation is extensive. Further, the model calculations involve multidimensional integrals, which are cumbersome to be evaluated, even if one uses simple Gaussian forms for the nuclear densities and nucleon-nucleon (NN) scattering amplitudes. Using the theory of permutation group, Yin *et al.* [11] have introduced a method to classify the multiple-scattering terms into sets; each set contains the terms of equal contribution to the scattering amplitude. As a result, these terms of equal contribution are represented by one typical term, named "orbit", and their number is referred to as the length of the corresponding orbit. The Gaussian forms for the nuclear densities and NN scattering amplitudes transform the multiple integral of each orbit into simple algebraic recurrence formulas. However, it has been proven

[a] e-mail: ali@mailer.eun.eg

that the classification method is practically useful only for calculating the full Glauber series of the multiple scattering between two composite systems of mass numbers $\leqslant$ 4 [12–14]. Recently, El-Gogary *et al.* have used the cluster approach [15] to extend the application of Yin's method to classify the multiple-scattering terms of heavier systems [16,17] and treated the center-of-mass correlations of such systems in a consistent manner [18]. The formulas developed in such attempts are practical approximations to the exact Glauber series calculation, but their applications show unsatisfactory descriptions for elastic collisions at medium energies. However, such disagreement was attributed to the inaccuracy of the NN parameters used at medium energies, and the simple Gaussian approximation for the NN amplitude, which is usually taken at high energies.

The aim of the present work is to test the reliability of these formulas for the scattering between two composite systems at higher energies, where the input NN data are available with sufficient accuracy [19–22]. For this purpose, many investigations have shown that the precise description of the composite scattering at high energy requires the consideration of quarks as substructure units inside the participating nucleons [23–26]. The Glauber model calculations [23] incorporating such role, have been carried out to investigate the proton-proton, proton-alpha and alpha-alpha elastic scattering at very high energies. The author in this attempt has truncated the multiple scattering between quarks up to the fifth order and parameterized the quark-quark (QQ) scattering amplitudes and the quark density with Gaussian forms. As an extension, we shall adopt the analysis developed by El-Gogary *et al.* in ref. [18] to obtain the quark model calculations for the composite scattering. The resulting formulas are given in sect. 2. The influence of a global momentum-dependent phase in the elemental scattering amplitudes is involved in this analysis. The results of the differential cross-sections of the proton-proton and proton-alpha interactions using this study and the discussion of the results are given in sect. 3. Concluding remarks are given is sect. 4. The orbits, lengths and the matrices required for the calculations are exhibited in the appendix.

2 Theory

In this section, the full Glauber series analysis of the elastic scattering between two composite systems having a cluster structure is presented. Each nucleon of the composite systems is taken as a cluster of three quarks. The Glauber theory is based on the eikonal and adiabatic approximations. In this theory, the elastic-scattering amplitude between two composite systems of mass numbers A and B may be written as [9]

$$F_{AB}\left(\vec{q}\right) = \frac{ik}{2\pi}\Theta\left(\vec{q}\right)\int \mathrm{d}\vec{b}\exp\left(i\vec{q}\cdot\vec{b}\right)\left\{1-\exp\left[i\chi_{AB}\left(\vec{b}\right)\right]\right\} \tag{1}$$

$$= \frac{ik}{2\pi}\int \mathrm{d}\vec{b}\exp\left(i\vec{q}\cdot\vec{b}\right)\left\{1-\exp\left[i\bar{\chi}_{AB}\left(\vec{b}\right)\right]\right\}, \tag{2}$$

where $\vec{q}$ is the momentum transferred from the projectile A to the target B, $\vec{k}$ is the incident momentum of the projectile, and $\vec{b}$ is the impact parameter vector. $\Theta\left(\vec{q}\right)$ is the global correction arising from the effect of the center-of-mass correlations [9]. $\bar{\chi}_{AB}\left(\vec{b}\right)$ stands for the nuclear phase shift function containing such correction consistently (the center-of-mass correlations are treated with the same order as the phase shift expansion) and it is related to the uncorrelated one, $\chi_{AB}\left(\vec{b}\right)$ by [7,9]

$$\exp\left(\, i\bar{\chi}_{AB}\left(\vec{b}\right)\,\right) = \int_0^\infty J_0(qb)\;\Theta(\vec{q})\;q\,\mathrm{d}q$$

$$\times\int_0^\infty J_0(qb')\;\exp\left(i\chi_{AB}\left(\vec{b}'\right)\right)\;b'\mathrm{d}b'\,. \tag{3}$$

Using the additivity assumption in the Glauber approximation [8], the total phase shift function χ_{AB} resulting from the interaction between the constituent particles can be related to the elemental phase shifts, χ_{ij} as,

$$\chi_{AB}\left(\vec{b},\{\vec{s}_i\},\{\vec{s}'_j\}\right) = \sum_{i=1}^{A}\sum_{j=1}^{B}\chi_{ij}\left(\vec{b}+\vec{s}_i-\vec{s}'_j\right) \tag{4}$$

and is given by

$$\exp\left(i\chi_{AB}\left(\vec{b}\right)\right) = \left\langle\,\Psi_A\Big(\{\vec{r}_i\}\Big)\Psi_B\Big(\{\vec{r}'_j\}\Big)\,\right|$$
$$\times\exp\left(i\chi_{AB}\left(\vec{b},\{\vec{s}_i\},\{\vec{s}'_j\}\right)\right)\;\left|\Psi_A\Big(\{\vec{r}_i\}\Big)\Psi_B\Big(\{\vec{r}'_j\}\Big)\,\right\rangle, \tag{5}$$

where, $\Psi_A\left(\{\vec{r}_i\}\right)$, $\left(\Psi_B\left(\{\vec{r}'_j\}\right)\right)$ is the ground-state wave function of the projectile (target) system, $\vec{s}_i$ $\left(\vec{s}'_j\right)$ is the projection of the relative position vector $\vec{r}_i$ $\left(\vec{r}'_j\right)$ of the i-th projectile (j-th target) particle (nucleon) on the impact parameter plane. The definition of the profile function is

$$\Gamma_{AB}\left(\vec{b}\right) = 1 - \exp\left[\, i\chi_{AB}\left(\vec{b}\right)\,\right],$$

the nuclear phase shift operator takes the form,

$$\exp\left(i\chi_{AB}\left(\vec{b},\{\vec{s}_i\},\{\vec{s}'_j\}\right)\right) =$$
$$\prod_{i=1}^{A}\prod_{j=1}^{B}\left[\,1-\Gamma_{ij}\left(\vec{b}+\vec{s}_i-\vec{s}'_j\right)\,\right], \tag{6}$$

where $\Gamma_{ij}\left(\vec{b}+\vec{s}_i-\vec{s}'_j\right)$ represents the profile function of the two-nucleon scattering. Expanding the products in eq. (6) gives the Glauber series representing the multiple scattering between the constituents of the interacting composite system. The number of terms contained in the series is $\left(2^{A\times B}-1\right)$; each term represents the multiple scattering with specific order. For practical calculations, let us follow the approach employed in ref. [18]. In this

approach the cluster structure of the colliding systems is considered. Suppose there are M_A clusters (nucleons) in system A and M_B clusters (nucleons) in system B, and there are M_N particles (quarks) in each cluster (M_N is a common divisor of A and B). Under this treatment, eq. (6) is re-expressed as

$$\exp\left(i\chi_{AB}\left(\vec{b},\{\vec{s}_{i\alpha}\},\{\vec{s}'_{j\delta}\}\right)\right) = \prod_{i=1}^{M_A}\prod_{j=1}^{M_B}\left[1-\Gamma_{ij}\left(\vec{b},\{\vec{s}_{i\alpha}\},\{\vec{s}'_{j\delta}\}\right)\right] \quad (7)$$

with

$$\Gamma_{ij}\left(\vec{b},\{\vec{s}_{i\alpha}\},\{\vec{s}'_{j\delta}\}\right) = 1-\prod_{\alpha=1}^{M_N}\prod_{\delta=1}^{M_N}\left[1-\Gamma_{i\alpha,j\delta}\left(\vec{b}+\vec{s}_{i\alpha}-\vec{s}'_{j\delta}\right)\right], \quad (8)$$

where Γ_{ij} represents the profile function of scattering between the i-th cluster in projectile A and j-th cluster in target B, while $\Gamma_{i\alpha,j\delta}$ is that between the α-th particle of the i-th cluster in A and the δ-th particle of j-th cluster in B.

Adopting the method of Yin *et al.* [11], we can classify the multiple-scattering terms of eq. (7) into sets; each one contains the terms of equal contribution to the scattering amplitude. All terms in each set are represented by one typical term, referred to as an orbit, and the number of terms in this set is referred to as the length of that orbit. Having utilized this classification, the nuclear phase shift takes the form

$$\begin{aligned}\exp\left(i\chi_{AB}\left(\vec{b},\{\vec{s}_{i\alpha}\},\{\vec{s}'_{j\delta}\}\right)\right) &= \left[1+\sum_{V_1=1}^{M_1}\sum_{\lambda_{V_1}}T_1\left(V_1,\lambda_{V_1}\right)\prod_{i=1}^{M_A}\prod_{j=1}^{M_B}\left[-\Gamma_{ij}\right]\right]^{\Delta_{ij}\left(V_1,\lambda_{V_1}\right)}\\ &= 1+\sum_{V_1=1}^{M_1}\sum_{\lambda_{V_1}}T_1\left(V_1,\lambda_{V_1}\right)\prod_{i=1}^{M_A}\prod_{j=1}^{M_B}\\ &\quad\times\left[\sum_{V_2=1}^{M_2}\sum_{\lambda_{V_2}}T_2\left(V_2,\lambda_{V_2}\right)\right.\\ &\quad\left.\times\prod_{\alpha=1}^{M_N}\prod_{\delta=1}^{M_N}\left[-\Gamma_{i\alpha,j\delta}\right]^{\Delta_{i\alpha,j\delta}\left(V_2,\lambda_{V_2}\right)}\right]^{\Delta_{ij}\left(V_1,\lambda_{V_1}\right)}, \end{aligned} \quad (9)$$

where $M_1 = M_A \times M_B$, $M_2 = M_N \times M_N$, and the indices (V,λ_V) characterize an orbit with order of scattering V and serial index λ_V. Each orbit (V_1,λ_{V_1}) for clusters ((V_2,λ_{V_2}) for particles in the clusters) is represented by a $M_A \times M_B$ ($M_N \times M_N$)-dimensional matrix, each of its elements $\Delta_{ij}\left(V_1,\lambda_{V_1}\right)$ ($\Delta_{i\alpha,j\delta}\left(V_2,\lambda_{V_2}\right)$) takes either the value *one*, if Γ_{ij} ($\Gamma_{i\alpha,j\delta}$) appears in the expansion term or *zero* if it is absent.

$T_1\left(V_1,\lambda_{V_1}\right)$ ($T_2\left(V_2,\lambda_{V_2}\right)$) is the length of the orbit $\left(V_1,\lambda_{V_1}\right)$ ($\left(V_2,\lambda_{V_2}\right)$) which is determined by using the properties of the permutation group, $G_1 = S_{M_A} \otimes S_{M_B}$ ($G_2 = S_{M_N} \otimes S_{M_N}$).

The scattering amplitude $f_{i\alpha,j\delta}\left(\vec{q}\right)$ is related to the profile function $\Gamma_{i\alpha,j\delta}\left(\vec{b}\right)$ by

$$\Gamma_{i\alpha,j\delta}\left(\vec{b}\right) = \frac{1}{2\pi\, ik_N}\int \mathrm{d}\vec{q}\exp\left(-\vec{q}\cdot\vec{b}\right) f_{i\alpha,j\delta}\left(\vec{q}\right). \quad (10)$$

Assuming, for simplicity, that all the two-particle amplitudes are identical, (which is approximately true at high energies) and neglecting any spin effects, $f_{i\alpha,j\delta}\left(\vec{q}\right)$ can be parameterized by [12,13,27,28],

$$f_{i\alpha,j\delta}\left(\vec{q}\right) = \frac{k_N\sigma}{4\pi}\left(i+\varepsilon\right)\exp\left(-\mu\, q^2/2\right), \quad (11)$$

where k_N is the momentum of the incident particle, σ is the particle-particle total cross-section, and ε is the ratio of the real to the imaginary parts of the forward-scattering amplitude. μ is taken to be complex $= \beta^2 + i\gamma^2$, where β^2 is the slope parameter of the elastic-scattering differential cross-section, and γ^2 is a free parameter introducing a phase variation of the elemental scattering amplitude.

Inserting eq. (11) into eq. (10) and performing the integration yields

$$\Gamma_{i\alpha,j\delta}\left(\vec{b}+\vec{s}_{i\alpha}-\vec{s}'_{j\delta}\right) = g\ \exp\left[-\left(\vec{b}+\vec{s}_{i\alpha}-\vec{s}'_{j\delta}\right)^2/2\mu\right], \quad (12)$$

where

$$g = \frac{\sigma}{4\pi\,\mu}\left(1-i\varepsilon\right).$$

Substituting eq. (12) into eq. (9) we get

$$\begin{aligned}\exp\left(i\chi_{AB}\left(\vec{b},\{\vec{s}_{i\alpha}\},\{\vec{s}'_{j\delta}\}\right)\right) &= 1+\sum_{V_1=1}^{M_1}\sum_{\lambda_{V_1}}T_1\ \left(V_1,\lambda_{V_1}\right)\\ &\times\prod_{i=1}^{M_A}\prod_{j=1}^{M_B}\left\{\sum_{V_2=1}^{M_2}\sum_{\lambda_{V_2}}T_2\ \left(V_2,\lambda_{V_2}\right)\ \left(-g\right)^{V_2}\exp\left[-\frac{1}{2\mu}\right.\right.\\ &\left.\left.\times\sum_{\alpha=1}^{M_N}\sum_{\delta=1}^{M_N}\left(\vec{b}+\vec{s}_{i\alpha}-\vec{s}'_{j\delta}\right)^2\Delta_{i\alpha,j\delta}\left(V_2,\lambda_{V_2}\right)\right]\right\}^{\Delta_{ij}\left(V_1,\lambda_{V_1}\right)}, \end{aligned} \quad (13)$$

where $V_2 = \sum_{\alpha=1}^{M_N}\sum_{\delta=1}^{M_N}\Delta_{i\alpha,j\delta}\left(V_2,\lambda_{V_2}\right)$.

Now we need to describe the wave function of the system to perform the integration of eq. (5). Consider the approximation in which the particles inside any cluster and the clusters themselves inside the system are completely uncorrelated. Then, we can write

$$\left|\Psi_A\left(\{\vec{r}_{i\alpha}\}\right)\Psi_B\left(\{\vec{r}'_{j\delta}\}\right)\right|^2 = \prod_{i=1}^{M_A}\prod_{\alpha=1}^{M_N}\rho_A\left(\vec{r}_{i\alpha}\right)\prod_{j=1}^{M_B}\prod_{\delta=1}^{M_N}\rho_B\left(\vec{r}'_{j\delta}\right), \quad (14)$$

where $\rho_A(\vec{r}_{i\alpha})$ and $\rho_B(\vec{r}'_{j\delta})$ are the normalized single-particle density functions and are chosen to be the single-Gaussian form,

$$\rho_\nu(\vec{r}) = (E_\nu)^{3/2} \exp\left(-\eta_\nu^2 r^2\right), \tag{15}$$

where $E_\nu = \eta_\nu^2/\pi$ and η_ν^2 is a size parameter related to the mean square radius $\langle r_\nu^2 \rangle$ of the nucleus $\nu = A$ or B. Because the incident direction of the projectile A is chosen to be the z-axis and $\chi_{AB}\left(\vec{b}\right)$ has no dependence on such variable in Glauber approximation, the integration of the nuclear densities in eq. (14) over the variables $z_{i\alpha}$ and $z'_{j\delta}$ in eq. (5) is straightforward and the transverse densities are

$$\left|\Psi_A\left(\{\vec{s}_{i\alpha}\}\right)\Psi_B\left(\{\vec{s}'_{j\delta}\}\right)\right|^2 = \prod_{i=1}^{M_A}\prod_{j=1}^{M_B}\left[C_A C_B \times \exp\left(-\sum_{\alpha=1}^{M_N}\eta_A^2 s_{i\alpha}^2 - \sum_{\delta=1}^{M_N}\eta_B^2 s'^2_{j\delta}\right)\right], \tag{16}$$

where

$$C_A = (E_A)^{M_N} \quad \text{and} \quad C_B = (E_B)^{M_N}.$$

With the phase function (13), the density (16), and the differential element

$$\mathrm{d}\tau = \prod_{i=1}^{M_A}\prod_{j=1}^{M_A}\left[\left(\prod_{\alpha=1}^{M_N}\mathrm{d}s_{i\alpha}\right)\left(\prod_{\delta=1}^{M_N}\mathrm{d}s'_{j\delta}\right)\right] = \prod_{i=1}^{M_A}\prod_{j=1}^{M_A}\left[\left(\prod_{\alpha=1}^{M_N}\mathrm{d}x_{i\alpha}\mathrm{d}y_{i\alpha}\right)\left(\prod_{\delta=1}^{M_N}\mathrm{d}x'_{j\delta}\mathrm{d}y'_{j\delta}\right)\right], \tag{17}$$

eq. (5) becomes

$$\exp\left(i\chi_{AB}\left(\vec{b}\right)\right) = 1 + \sum_{V_1=1}^{M_1}\sum_{\lambda_{V_1}} T_1\ (V_1,\lambda_{V_1}) \times \prod_{i=1}^{M_A}\prod_{j=1}^{M_B}\left[C_A C_B \sum_{V_2=1}^{M_2}\sum_{\lambda_{V_2}} T_2(V_2,\lambda_{V_2})\ (-g)^{V_2} \times \int\left(\prod_{\alpha=1}^{M_N}\mathrm{d}s_{i\alpha}\right)\left(\prod_{\delta=1}^{M_N}\mathrm{d}s'_{j\delta}\right)\exp\left\{-\sum_{\alpha=1}^{M_N}\eta_A^2 s_{i\alpha}^2 - \sum_{\delta=1}^{M_N}\eta_B^2 s'^2_{j\delta} - \frac{1}{2\mu}\sum_{\alpha=1}^{M_N}\sum_{\delta=1}^{M_N}\left(\vec{b}+\vec{s}_{i\alpha}-\vec{s}'_{j\delta}\right)^2 \times \Delta_{i\alpha,j\delta}\ (V_2,\lambda_{V_2})\right\}\right]^{\Delta_{ij}(V_1,\lambda_{V_1})}. \tag{18}$$

This equation can be rewritten as

$$\exp\left(\ i\chi_{AB}\left(\vec{b}\right)\right) = 1 + \sum_{V_1=1}^{M_1}\sum_{\lambda_{V_1}} T_1\ (V_1,\lambda_{V_1}) \times \prod_{i=1}^{M_A}\prod_{j=1}^{M_B}\left[C_A C_B \sum_{V_2=1}^{M_2}\sum_{\lambda_{V_2}} T_2(V_2,\lambda_{V_2})\ (-g)^{V_2} \times J_{\left(V_2,\lambda_{V_2},\Delta_{i\alpha,j\delta}(V_2,\lambda_{V_2})\right)}\left(\vec{b}\right)\right]^{\Delta_{ij}(V_1,\lambda_{V_1})}, \tag{19}$$

where

$$J_{\left(V_2,\lambda_{V_2},\Delta_{i\alpha,j\delta}(V_2,\lambda_{V_2})\right)}\left(\vec{b}\right) = \int\left(\prod_{\alpha=1}^{M_N}\mathrm{d}s_{i\alpha}\right)\left(\prod_{\delta=1}^{M_N}\mathrm{d}s'_{j\delta}\right) \times \exp\left\{-\sum_{\alpha=1}^{M_N}\eta_A^2 s_{i\alpha}^2 - \sum_{\delta=1}^{M_N}\eta_B^2 s'^2_{j\delta} - \frac{1}{2\mu}\sum_{\alpha=1}^{M_N}\sum_{\delta=1}^{M_N}\left(\vec{b}+\vec{s}_{i\alpha}-\vec{s}'_{j\delta}\right)^2 \Delta_{i\alpha,j\delta}(V_2,\lambda_{V_2})\right\}. \tag{20}$$

The multiple integral in eq. (20) can be solved recursively yielding the result

$$J_{\left(V_2,\lambda_{V_2},\Delta_{i\alpha,j\delta}(V_2,\lambda_{V_2})\right)}\left(\vec{b}\right) = R\left(V_2,\lambda_{V_2},\Delta_{i\alpha,j\delta}(V_2,\lambda_{V_2})\right) \times \exp\left[-S\ (V_2,\lambda_{V_2},\Delta_{i\alpha,j\delta}(V_2,\lambda_{V_2}))\ b^2\right] \tag{21}$$

with

$$R\ (V_2,\ \lambda_{V_2},\Delta_{i\alpha,j\delta}(V_2,\lambda_{V_2})) = \left[\prod_{\alpha=1}^{M_N}\left(4\pi\mu^2 T_\alpha(i,j,V_2,\lambda_{V_2})\right)\right]\left[\prod_{\delta=1}^{M_N}\left(\frac{\pi}{a_{\delta\delta}\ (i,j,\delta)}\right)\right] \tag{22}$$

and

$$S\left(V_2,\ \lambda_{V_2},\Delta_{i\alpha,j\delta}(V_2,\lambda_{V_2})\right) = a_0\ (\delta) - \sum_{\delta=1}^{M_N}\frac{c_\delta^2(\delta)}{4a_{\delta\delta}\ (i,j,\delta)}. \tag{23}$$

The different symbols appearing in eqs. (22), (23) are defined below:

$$T_\alpha(i,j,V_2,\lambda_{V_2}) = 1/2\mu\left(2\mu\,\eta_A^2 + \rho_\alpha(i,j,V_2,\lambda_{V_2})\right), \tag{24}$$

where

$$\rho_\alpha(i,j,V_2,\lambda_{V_2}) = \sum_{\delta=1}^{M_N}\Delta_{i\,\alpha,j\delta}(V_2,\lambda_{V_2}),$$

and the a's and c's coefficients are determined by using the simple algebraic recursion formulas:

$$a_0(M_N) = \sum_{\delta=1}^{M_N}\eta_B^2,$$

$$a_{\delta\delta}(i,j,M_N) = \eta_B^2 + \frac{1}{2\mu}\sigma_\delta(i,j,V_2,\lambda_{V_2}) - \sum_{\alpha=1}^{M_N}T_\alpha(i,j,V_2,\lambda_{V_2})\,\Delta_{i\alpha,j\delta}(V_2,\lambda_{V_2}),$$

where

$$\sigma_\delta(i,j,V_2,\lambda_{V_2}) = \sum_{\alpha=1}^{M_N}\Delta_{i\,\alpha,j\delta}(V_2,\lambda_{V_2}),$$

$$a_{\delta\beta}(i,j,M_N) = 2\sum_{\alpha=1}^{M_N}T_\alpha(i,j,V_2,\lambda_{V_2})\,\Delta_{i\alpha,j\delta}(V_2,\lambda_{V_2}) \times\Delta_{i\alpha,j\beta}(V_2,\lambda_{V_2}), \qquad \beta>\delta$$

$$c_\delta(M_N) = 2\eta_B^2, \tag{25}$$

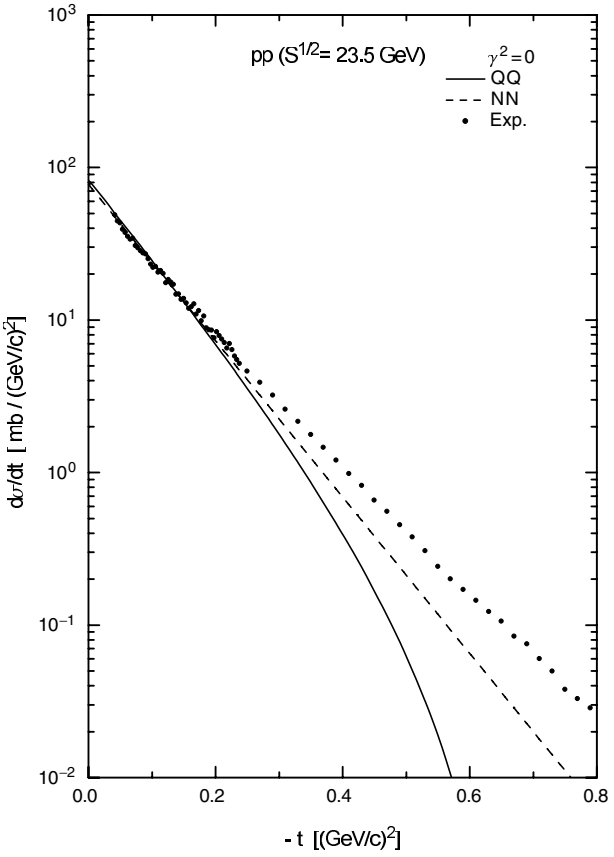

Fig. 1. Full Grauber series calculation of the elastic differential cross-section for pp collision at center-of-mass energy 23.5 GeV, with no phase variation for the QQ and NN models compared to the experimental data, ref. [19].

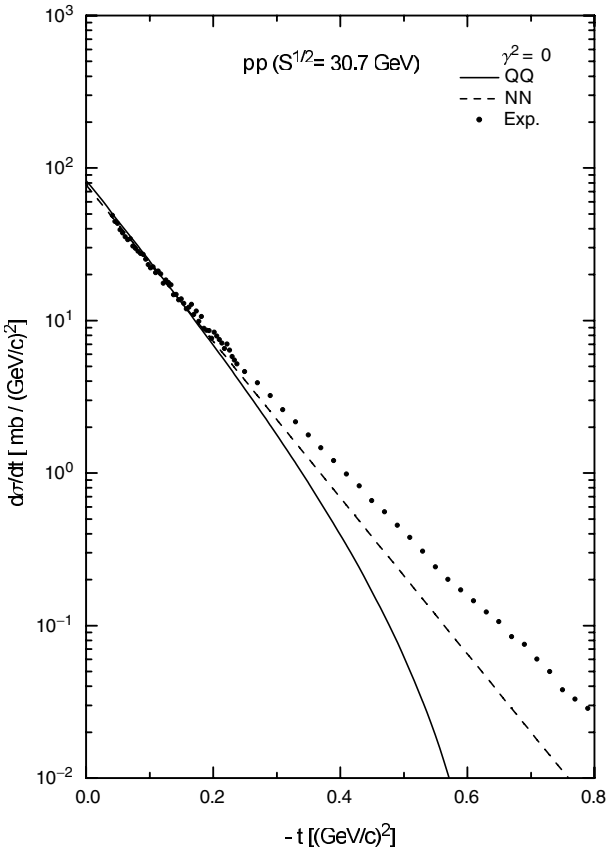

Fig. 2. As in fig. 1 but for the center-of-mass energy 30.7 GeV.

$$a_{\delta\delta}\left(i,j,M_N-1\right)=a_{\delta\delta}\left(i,j,M_N\right)-\frac{a^2_{\delta M_N}\left(i,j,M_N\right)}{4a_{M_NM_N}(i,j,M_N)},$$

$$a_{\delta\beta}\left(i,j,M_N-1\right)=a_{\delta\beta}\left(i,j,M_N\right)+\frac{a_{\delta\,M_N}\left(i,j,M_N\right)\,a_{\beta M_N}\left(i,j,M_N\right)}{2a_{M_NM_N}\left(i,j,M_N\right)},\qquad \beta>\delta$$

$$c_\delta\left(M_N-1\right)=c_\delta\left(M_N\right)+\frac{c_{M_N}\left(M_N\right)a_{\delta M_N}\left(i,j,M_N\right)}{2a_{M_NM_N}\left(i,j,M_N\right)}.$$

The details of the integration method are illustrated in ref. [15], according to which, we get

$$\exp\left(i\chi_{AB}\left(\vec{b}\right)\right)=1+\sum_{V_1=1}^{M_1}\sum_{\lambda_{V_1}}T_1\left(V_1,\lambda_{V_1}\right)\prod_{i=1}^{M_A}\prod_{j=1}^{M_B}\left[C_AC_B\times\sum_{V_2=1}^{M_2}\sum_{\lambda_{V_2}}T_2\left(V_2,\lambda_{V_2}\right)(-g)^{V_2}R\left(V_2,\lambda_{V_2},\Delta_{i\alpha,j\delta}\left(V_2,\lambda_{V_2}\right)\right)\times\exp\left\{-S\left(V_2,\lambda_{V_2},\Delta_{i\alpha,j\delta}\left(V_2,\lambda_{V_2}\right)\right)b^2\right\}\right]^{\Delta_{ij}\left(V_1,\lambda_{V_1}\right)}. \tag{26}$$

Incorporation of the center-of-mass correlation in the phase shift function is performed in the following way:

$$\exp\left(i\chi_{AB}\left(\vec{b}\right)\right)=1+\sum_{V_1=1}^{M_1}\sum_{\lambda_{V_1}}T_1\left(V_1,\lambda_{V_1}\right)\prod_{i=1}^{M_A}\prod_{j=1}^{M_B}\left[Z\right]^{\Delta_{ij}\left(V_1,\lambda_{V_1}\right)}, \tag{27}$$

where

$$Z=\;C_AC_B\sum_{V_2=1}^{M_2}\sum_{\lambda_{V_2}}T_2\left(V_2,\lambda_{V_2}\right)\;(-g)^{V_2}\times R\left(V_2,\lambda_{V_2},\Delta_{i\alpha,j\delta}\left(V_2,\lambda_{V_2}\right)\right)\times\exp\left[-S\left(V_2,\lambda_{V_2},\Delta_{i\alpha,j\delta}\left(V_2,\lambda_{V_2}\right)\right)b^2\right]. \tag{28}$$

The modified phase shift function $\bar{\chi}_{AB}\left(\vec{b}\right)$ (cf. eq. (2)) can be similarly written as

$$\exp\left(i\bar{\chi}_{AB}\left(\vec{b}\right)\right)=1+\sum_{V_1=1}^{M_1}\sum_{\lambda_{V_1}}T_1\left(V_1,\lambda_{V_1}\right)\prod_{i=1}^{M_A}\prod_{j=1}^{M_B}\left[\bar{Z}\right]^{\Delta_{ij}\left(V_1,\lambda_{V_1}\right)}. \tag{29}$$

Table 1. The parameters of the QQ and NN scattering amplitudes are taken from the references stated in the table.

$\sqrt{s}$ (GeV)	σ (fm^2)		ε		β^2 (fm^2)		Ref. No.	
	σ_{QQ}	σ_{NN}	ε_{QQ}	ε_{NN}	β^2_{QQ}	β^2_{NN}	QQ	NN
23.5	0.535	3.894	0.11	0.02	0.07383	0.4595	[13]	[19]
30.7	0.5352	4.014	0.045	0.037	0.083	0.47505	[23]	[22]
44.7	0.5555	4.179	0.075	0.062	0.105	0.4984	[23]	[19]
52.8	0.5555	4.267	0.075	0.078	0.105	0.501	[23]	[19]

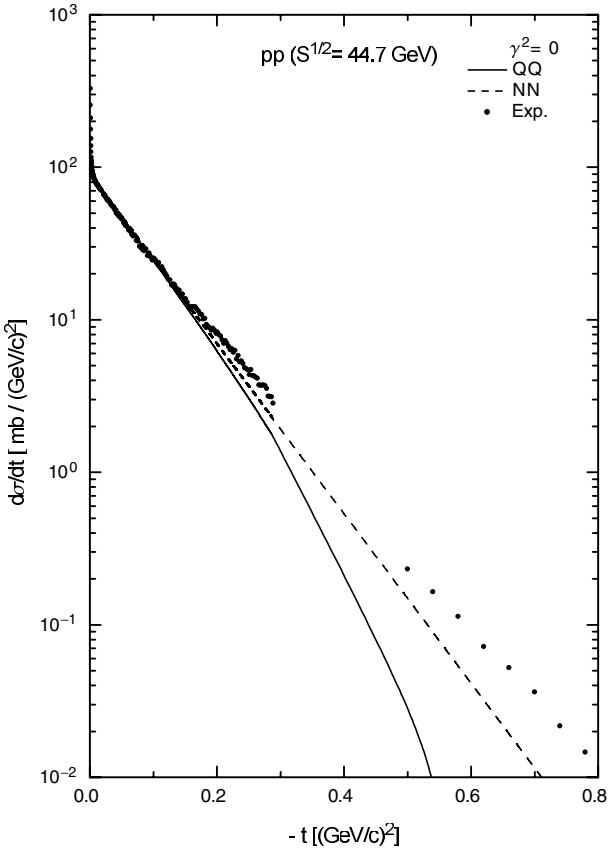

Fig. 3. As in fig. 1 but for the center-of-mass energy 44.7 GeV.

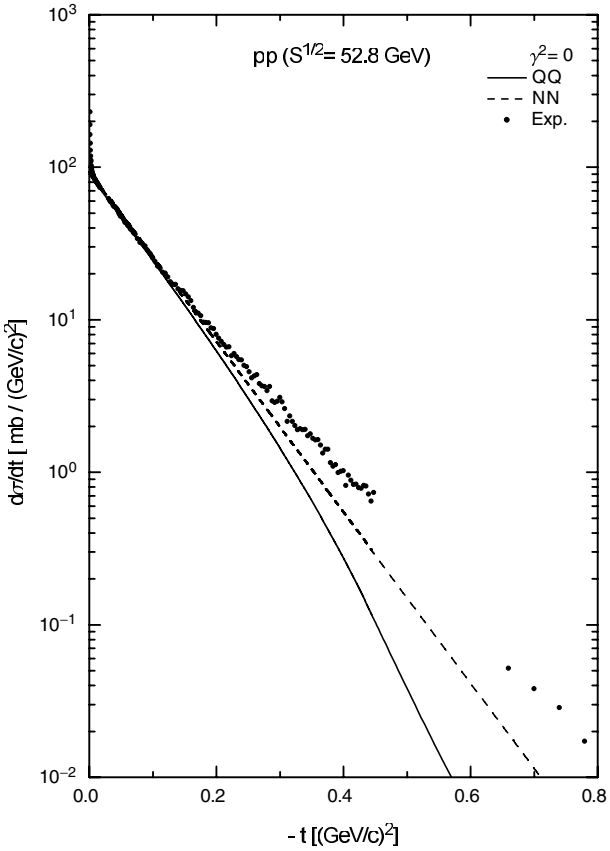

Fig. 4. As in fig. 1 but for the center-of-mass energy 52.8 GeV.

Inserting the expression of Z and the factor of the center-of-mass correction [10],

$$\Theta\left(\vec{q}\right) = \exp\left[\frac{q^2}{4}\left(\frac{1}{A\eta_A^2} + \frac{1}{B\eta_B^2}\right)\right]$$

into eq. (2) leads, for $\bar{Z}$, to

$$\begin{aligned}\bar{Z} = C_A\, C_B \sum_{V_2=1}^{M_2} \sum_{\lambda_{V_2}} & T_2\ (V_2,\, \lambda_{V_2})\ \ (-g)^{\ V_2} \\ & \times \bar{R}\ (V_2, \lambda_{V_2}, \Delta_{i\alpha,j\delta}\,(V_2, \lambda_{V_2})\,) \\ & \times \exp\left[-\bar{S}\,(V_2,\, \lambda_{V_2},\, \Delta_{i\alpha,j\delta}\,(V_2, \lambda_{V_2})\,)\ b^2\right] \end{aligned} \tag{30}$$

with

$$\bar{S} = \left[\frac{1}{S} - \frac{1}{A\eta_A^2} - \frac{1}{B\eta_B^2}\right]^{(-1)} \quad \text{and} \quad \bar{R} = \frac{R \times \bar{S}}{S}.$$

Using eqs. (29), (30), the scattering amplitude can be obtained by performing the integration in eq. (2). The integration is, in general, obtained numerically but if no clustering is used, *i.e.* $M_A = A$, $M_B = B$ and $M_N = 1$, it gives the following analytical result:

$$\begin{aligned} F_{AB}(\,q\,) = 1 \,+\, c_A\ c_B \Bigg\{ \sum_{V_1=1}^{M_1} \sum_{\lambda_{V_1}} & T_1\ (V_1,\, \lambda_{V_1})\ \ (-g)^{\ V_1} \\ & \times \frac{\bar{R}\ (V_1, \lambda_{V_1}, \Delta_{ij}\,(V_1, \lambda_{V_1})\,)}{2\ \bar{S}\ \ (V_1,\, \lambda_{V_1},\, \Delta_{ij}\,(V_1, \lambda_{V_1})\,)} \\ & \times \exp\left[-\frac{q^2}{4\,\bar{S}\ \ (V_1,\, \lambda_{V_1},\, \Delta_{ij}\,(V_1, \lambda_{V_1})\,)}\right]\Bigg\}, \end{aligned} \tag{31}$$

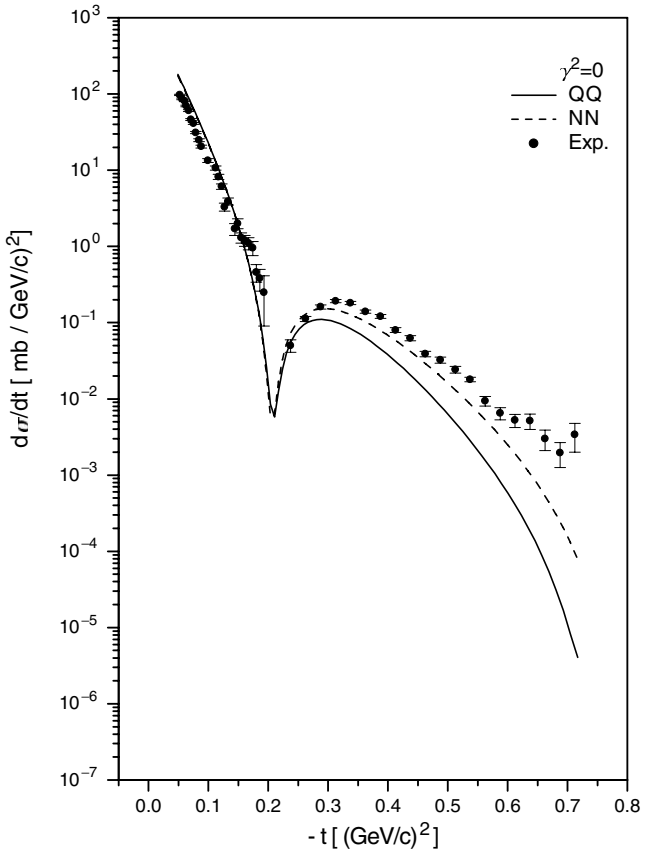

Fig. 5. Full Grauber series calculation of the elastic differential cross-section for αp collision at center-of-mass energy 88, 89 GeV, with no phase variation for the QQ and NN models compared to the experimental data, ref. [20].

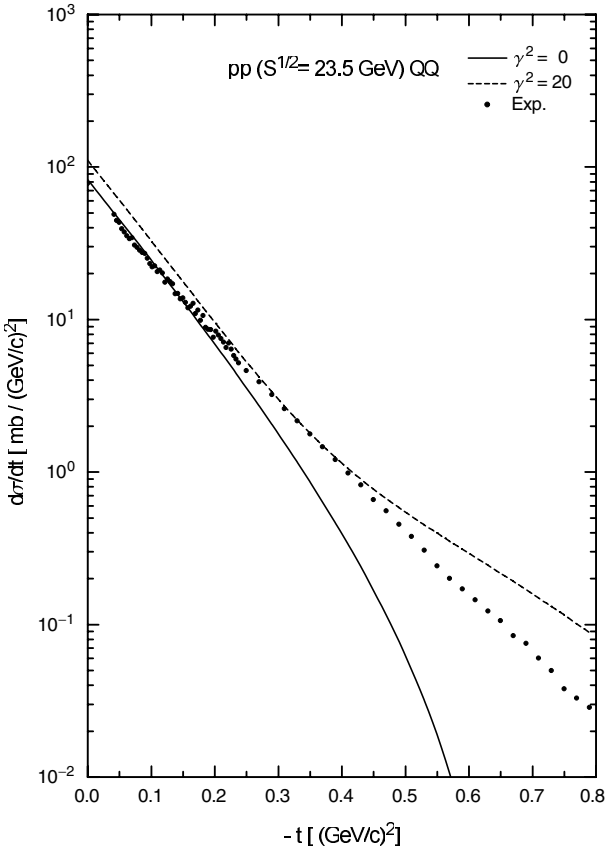

Fig. 6. As in fig. 1 but for the QQ model only with phase parameter $\gamma^2 = 20$ compared to that with $\gamma^2 = 0$.

where $V_1 = \sum_{i=1}^{M_A} \sum_{j=1}^{M_B} \Delta_{ij}\,(V_1, \lambda_{V_1})$.

The angular distribution of the elastic scattering is then given by,

$$\frac{\mathrm{d}\sigma\,(\vec{q})}{\mathrm{d}\Omega} = |F_{AB}\,(\vec{q})\,|^2. \tag{32}$$

3 Results and discussion

The composite-composite elastic collision is derived by considering the full Glauber series of the multiple scattering between their constituent nucleons as clusters of three quarks. The analytic formula for the nuclear phase shift function is developed using Gaussian parameterization for the QQ scattering amplitudes and the quark densities. The quark model application has been started by calculating the differential cross-section of the pp collisions, at very high energies, namely at center-of-mass energies $\sqrt{s} = 23.5$, 30.7, 44.7 and 52.8 GeV. The calculations are extended to αp collision at $\sqrt{s} = 88$ and 89 GeV. For comparison, the results of the conventional nucleon model are also calculated. The ingredients needed to perform these calculations are the parameters associated with the QQ and the NN scattering amplitudes σ, ε and β^2 (cf. eq. (11)) and the quark/nucleon densities η_A, η_B, cf. eq. (15). The QQ and NN parameters used here are listed in table 1 with the corresponding references from which they are taken. Those parameters are obtained by fitting the NN data at the corresponding energies.

The values of the η_ν parameters, corrected for the effects of the finite proton size and the c.m. recoil, are given by

$$\eta_\nu^2 = \frac{3}{2}\left(\frac{(1-1/\nu)}{\langle r_\nu^2\rangle - \langle r_{\mathrm{p}}^2\rangle}\right), \qquad \nu = A, B,$$

where $\langle r_\nu^2\rangle$ and $\langle r_{\mathrm{p}}^2\rangle$ are the mean square radii of the nucleus and the proton, respectively and their values are taken from ref. [22].

The numbers (M_A, M_B, M_N), determining the cluster structure assumed in each system, are taken as follows: For the pp case, the quark configuration is considered by taking $M_A = M_B = 1$, and $M_N = 3$, while for the nucleon configuration $M_A = M_B = M_N = 1$. For the αp case, the numbers for the quark configuration are $M_A = 4$, $M_B = 1$ and $M_N = 3$, while for the nucleon configuration they are $M_A = 4$, $M_B = 1$ and $M_N = 1$. The orbits, lengths and Δ-matrices of the groups $G_1 = S_{M_A} \otimes S_{M_B}$ and $G_2 = S_{M_N} \otimes S_{M_N}$ for the corresponding structures are exhibited in the appendix.

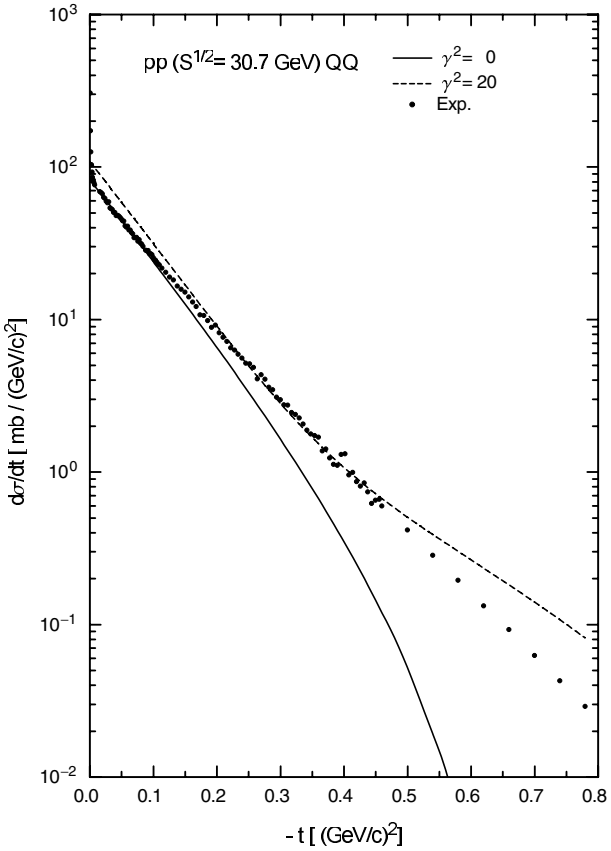

Fig. 7. As in fig. 6 but for the center-of-mass energy 30.7 GeV.

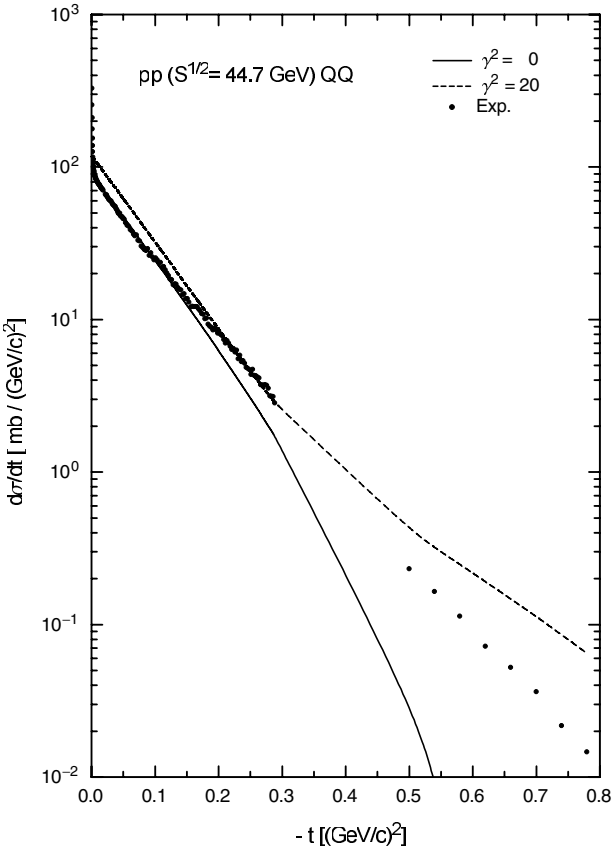

Fig. 8. As in fig. 6 but for the center-of-mass energy 44.7 GeV.

Figures 1, 2, 3, 4 show the differential cross-sections for the pp elastic scattering at $\sqrt{s}$ = 23.5, 30.7, 44.7 and 52.8 GeV, respectively. In these figures, the pp cross-sections obtained from the quark and nucleon structure calculations, with no phase variation (cf. eq. (11) and below), *i.e.* the parameter $\gamma^2 = 0$, are compared with the experimental data. We can see that the nucleon model results fit the experimental data better than the quark model calculations. The calculations obtained from the two models are nearly identical, and in good agreement with the scattering data over the range of momentum transfer $0.0 < -t < 0.2$ $(\mathrm{GeV}/c)^2$. Beyond the value 0.2 $(\mathrm{GeV}/c)^2$, the results obtained from the two models differ significantly, and show an advantage for the nucleon model over the quark one, and both are in disagreement with the experimental data. Also, the range of agreement with the experimental data decreases as the center-of-mass energy of the pp scattering increases.

The elastic differential cross-section for αp scattering at $\sqrt{s}$ = 89 and 88 GeV are shown in fig. 5, it displays the same trend as in the pp case. The results of the QQ and NN with no phase variation are almost identical, and fairly agree with the experimental data over the range of momentum transfer $0.05 < -t < 0.3$ $(\mathrm{GeV}/c)^2$. For $-t \geqslant 0.3$ $(\mathrm{GeV}/c)^2$, the nucleon model results show closer values to the experimental data than the quark model over the range $0.3 < -t \leqslant 0.7$ $(\mathrm{GeV}/c)^2$.

However, the present analysis has shown a better overall description for the elastic scattering between two composite systems at high energy than that found at medium energy [17,18] and improves slightly the previous QQ description considered in ref. [23].

Several authors [3,4,12,13], have obtained better fits by introducing a phase variation in the QQ and NN scattering amplitudes. To investigate the influence of such phase variation on the present calculations, the results of the differential cross-section at various nonzero values of the parameter γ^2, are calculated. The best fits are compared with the free phase calculations as shown in figs. 6-11.

Figures 6-9 show the phase variation effect in the pp elastic scattering via the quark structure at $\sqrt{s}$ = 23.5, 30.7, 44.7, 52.8 GeV, respectively. It is clear that the phase variation improves, in general, the agreement with the data, especially at large momentum transfer ($-t > 0.3$ $(\mathrm{GeV}/c)^2$). We have found that the best agreement at these energies is obtained with almost the same value of $\gamma^2 = 20$ $(\mathrm{GeV}/c)^2$, which is close to that reported in ref. [13]. This reflects that the energy dependence of γ^2 is weak in this energy range.

Figures 10, 11 show the phase variation effect in αp elastic-scattering cross-section at $\sqrt{s}$ = 88 and 89 GeV via quark structure and nucleon structure, respectively. As can be seen from these figures, the results obtained have similar improvements as in the case of pp collision.

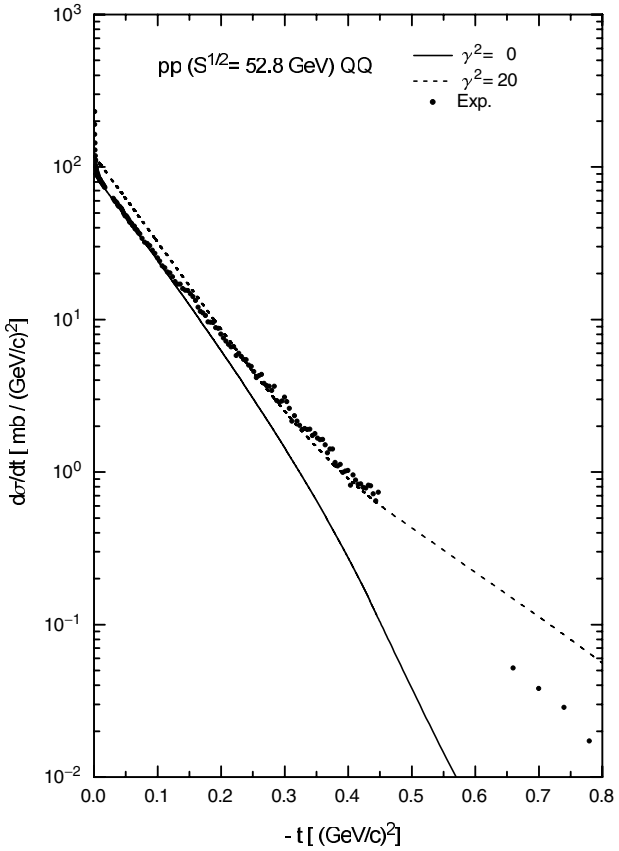

Fig. 9. As in fig. 6 but for the center-of-mass energy 52.8 GeV.

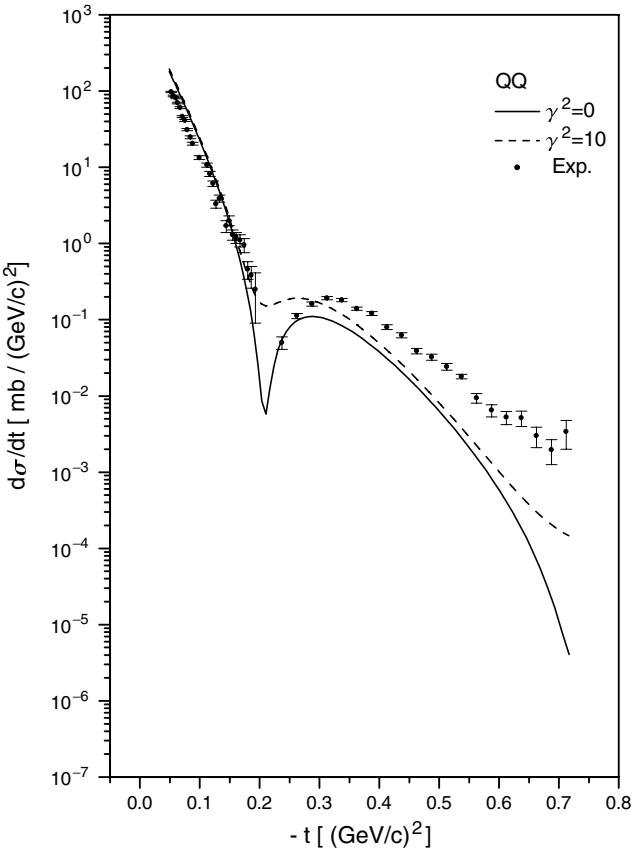

Fig. 10. The effect of phase variation on the elastic differential cross-section for αp collision via quark structure at center-of-mass energy 88, 89 GeV. Data are taken from ref. [20].

The calculation with value $\gamma^2 = 10$ $(\mathrm{GeV}/c)^2$ gives the best agreement with the scattering data for both models.

The phase variation has different effects on different momentum transfers, center-of-mass energies and colliding systems. In general, the elastic cross-section increases as γ^2 increased especially at large momentum transfer.

Although the introduction of phase variation has improved the overall agreement with experimental data, some disagreements still prevail at high momentum transfer.

The remaining disagreement may be due to the following:

i) The underestimation of the quark model prediction cross-section compared to that of the nucleon mode, at large values of momentum transfer, may be attributed to the large number of quark scattering centers, which may imply strong destructive interference.

ii) The simple Gaussian forms for the nuclear density and scattering amplitude do not account properly for the details of the nuclear density and the scattering amplitude in these interactions. Calculations with more realistic forms, such as the harmonic oscillator, may give more satisfactory agreement at large momentum transfer, although the input parameters of two models are weakly dependent on energy, as seen from table 1.

iii) The present analysis is performed for either the quark or the nucleon model over the whole range of the impact parameter, but one may argue that, different sections of this range should be treated with different models. M. Wei-hsing *et al.* [24,25] proposed a hybrid quark-hadron (HQH) model, in which the interaction between quarks is restricted to the range of impact parameter $b \leqslant 0.7$ fm, while the conventional NN interaction is considered in the exterior range $b > 0.7$ fm. They have applied their model to proton-alpha and alpha-alpha elastic scatterings, and have shown an improvement in the fitting with the experimental data for αp scattering at $-t > 0.3$ $(\mathrm{GeV}/c)^2$ [24], and slightly better results for $\alpha\alpha$ elastic scattering [25] than the pure QQ model calculations [23]. This fair success of the HQH model encourages further study of high-energy elastic scattering, but its generalization to more massive nuclei possesses mathematical difficulties to the present work formulation which has to be overcome.

4 Conclusion

The full Glauber multiple-scattering series theory is used to analyze the elastic proton-proton and alpha-proton collisions in the center-of-mass energy range 20–90 GeV. Two models of interaction are used, one is based on the nucleon-nucleon and the other on the quark-quark scattering. Phase variation is introduced in the calculation to evaluate its effect.

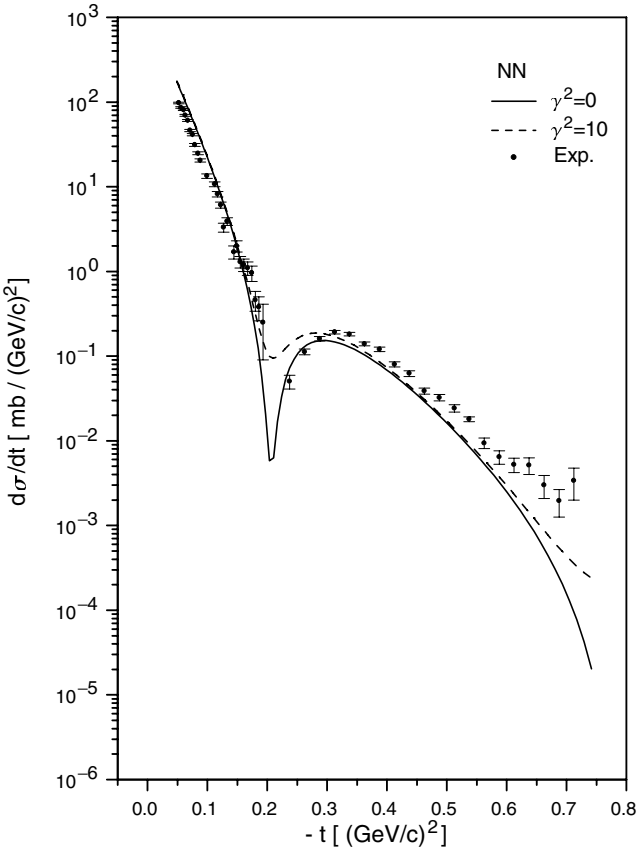

Fig. 11. As in fig. 10 but for αp collision via nucleon structure.

One can summarize the findings of the present study as follows:
i) The inclusion of the full Glauber series extends the applicability of the model at large momentum transfer, for both quark and nucleon structures. For high momentum transfer the nucleon model is better than the quark model.
ii) The agreement with the data for pp scattering for the two models seems to be energy independent.
iii) As the phase variation constant increases the cross-section increases, and it shows partial improvement for $\gamma^2 = 10$–20 fm^2.
iv) The increasing disagreement for more massive participants (αp) encourages the study of more realistic forms of the QQ/NN amplitude and nucleon density distributions.

Appendix A.

This appendix contains the tables of the orbits, lengths and Δ-matrices employed in our calculations. We obtained them by enumerating and investigating all the possible combinations of collisions according to their permutation [22]. In the preset work, the elastic collisions, pp and αp, have been studied under their quark and nucleon structures. The orbits, lengths and Δ-matrices of the groups $G_1 = S_{M_A} \otimes S_{M_B}$ and $G_2 = S_{M_N} \otimes S_{M_N}$ (defined in sect. 2) corresponding to these reactions depend on the assumed cluster configuration.

Table 2. Orbits, lengths and Δ-matrices for $G = S_4 \otimes S_1$. The total number of orbits (including the orbits not shown) is equal to 4.

V	λ_V	$T(V,\lambda_V)$	$\Delta(V,\lambda_V)$
1	1	4	1000
2	1	6	1100

Table 3. Orbits, lengths and Δ-matrices for $S_3 \otimes S_3$. The total number of orbits (including the orbits not shown) is equal to 25.

V	λ_V	$T(V,\lambda_V)$	$\Delta(V,\lambda_V)$
1	1	9	1 0 0 0 0 0 0 0 0
2	1	18	1 1 0 0 0 0 0 0 0
2	2	18	1 0 0 0 1 0 0 0 0
3	1	6	1 1 1 0 0 0 0 0 0
3	2	36	1 1 0 0 0 1 0 0 0
3	3	36	1 1 0 1 0 0 0 0 0
3	4	6	1 0 0 0 1 0 0 0 1
4	1	36	1 1 1 1 0 0 0 0 0
4	2	36	1 1 0 1 0 1 0 0 0
4	3	9	1 1 0 1 1 0 0 0 0
4	4	36	1 1 0 1 0 0 0 0 1
4	5	9	0 1 1 1 0 0 1 0 0

For the pp case, the quark cluster configuration yields $M_A = M_B = 1$ and $M_N = 3$, while the configuration in case of nucleon based structure gives $M_A = M_B = M_N = 1$. For the αp case, the quark cluster configuration is to be M_A= 4, $M_B = 1$ and $M_N = 3$, while the configuration in case of nucleon takes M_A= 4, $M_B = 1$ and $M_N = 1$.

For the sake of brevity, we give only the tables of the nonsimilar groups (see tables 2 and 3).

In these tables, the first column represents the order of multiple scattering V which ranges from 1 to $m \times n$ while λ_V, in the second column, represents the serial index used to number the orbits of order V. The third column represents the length of the orbit $T(V,\lambda_V)$. In the fourth column the $(m \times n)$-digit binary numbers give the Δ-matrices of the group $G = S_m \otimes S_n$. The first n-digits are the elements Δ_{1i}, $i = 1, 2, \ldots, n$; the next n-digits are Δ_{2i}, ..., and the last n-digits are Δ_{mi}. By symmetry, the orbits, lengths and Δ-matrices for V's which are not shown in our tables, could be easily deduced using the tables. This is carried out by using the results for order $V' = m \times n - V$ and interchanging the 0's and 1's of $\Delta(V', \lambda_{V'})$. The indices λ_V and $\lambda_{V'}$ are the same and the lengths $T(V,\lambda_V)$ and $T(V',\lambda_{V'})$ are equal. The matrix $\Delta(m \times n, 1)$ has elements Δ_{ij} equal to 1.

References

1. G. Fäldt, H. Pilkuhn, H.G. Sclaile, Ann. Phys. (N.Y.) **82**, 326 (1974); I.V. Andreev, A.V. Chernov, Sov. J. Nucl. Phys. **28**, 243 (1978); I.V. Andreev, L.A. Khein, Sov. J. Nucl. Phys. **28**, 770 (1978); A.P. Gasparian *et al.*, Nucl. Phys. **34**, 739 (1981); G.D. Alkhazov *et al.*, Nucl. Phys. A **280**, 365 (1977); S.D. Lenzi, A. Vitturi, F. Zardi, Phys. Rev. C **40**, 2114 (1989); J. Chauvin, D. Lebrun, A. Lounis, M. Buenerd, Phys. Rev. C **28**, 1970 (1983).

2. H.P. Morsch *et al.*, Z. Phys. A **350**, 167 (1994); G. Bartnitzky *et al.*, Phys. Lett. B **365**, 23 (1996).
3. Ji-feng Liu, Yu-shun Zhang, Chao-yun Yang, Jun-feng Shen, B.A. Robson, Phys. Rev. C **54**, 2509 (1996).
4. R.J. Lombard, J.P. Maillet, Phys. Rev. C **41**, R1348 (1990).
5. R.J. Glauber, *Lectures in Theoretical Physics*, edited by W.E. Brittin, L.G. Dunham, Vol. **1** (Wiley, New York, 1959) p. 315; V. Franco, R.J. Glauber, Phys. Rev. **142**, 1195 (1966); R.J. Glauber, V. Franco, Phys. Rev. **156**, 1685 (1967).
6. R.J. Glauber, G. Mathiae, Nucl. Phys. B **21**, 135 (1970); C. Wilikin, Nuovo Cimento Lett. **4**, 491 (1970); H. Lesniak, L. Lesniak, Nucl. Phys. B **38**, 221 (1972); J.P. Auger, R.J. Lombard, Phys. Lett. B **45**, 115 (1973); G. Igo, *High-Energy Physics and Nuclear Structure*, edited by D.E. Negle *et al.* (AIP, New York, 1975) p. 63; V. Franco, Phys. Rev. C **8**, 1690 (1974).
7. V. Franco, A. Tekou, Phys. Rev. C **16**, 658 (1977).
8. G.K. Varma, Nucl. Phys. A **294**, 465 (1978).
9. V. Franco, G.K. Varma, Phys. Rev. C **18**, 349 (1978).
10. W. Czyz, L.C. Maximon, Ann. Phys. (N.Y.) **52**, 59 (1969).
11. Yin Yichun, Tan Zhenqiang, Chen Kezhong, Nucl Phys. A **440**, 685 (1985); Y. Yin *et al.*, Chin. Phys. **6**, 93 (1986); Phys. Ener. Fort. Phys. Nucl. **9**, 569 (1985).
12. V. Franco, Y. Yin, Phys. Rev. C **34**, 608 (1986).
13. Zhen-Qiang Tan, Zheng-Jin Lin, Pan-Ning Yan, Chong-En Wu, J. Phys. G **16**, 1697 (1990).
14. Zong-Jin Lin, Shu-Xia Yu, Xiang Zhong Huang, Chong-En Wu, J. Phys. G **17**, 1159 (1991).
15. Huang Xiang Zhong, Phys. Rev. C **51**, 2700 (1995).
16. A.S. Shalaby, M.M.H. EL-Gogary, M.Y.M. Hassan, Phys. Rev. C **56**, 2889 (1997).
17. M.M.H. EL-Gogary, A.S. Shalaby, M.Y.M. Hassan, Phys. Rev. C **58**, 3513 (1998).
18. M.M.H. EL-Gogary, A.S. Shalaby, M.Y.M. Hassan, A.M. Hegazy, Phys. Rev. C **61**, 044604 (2000).
19. K.R. Schubert, *Tables on Nucleon-Nucleon Scattering*, Vol. **9** (Springer, New York, 1980) p. 273; U. Amaldi, K.R. Schubert, Nucl. Phys. B **166**, 301 (1980);
20. M. Ambroso *et al.*, Phys. Lett. B **113**, 347 (1982); W. Bell *et al.*, Phys. Lett. B **117**, 131 (1982).
21. L. Setta *et al.*, Phys. Lett. B **139**, 263 (1984).
22. N. Amos *et al.*, Nucl. Phys. B **262**, 689 (1985).
23. V. Franco, Phys. Rev. C **35**, 1328 (1987).
24. Ma Wei-hsing, Huang Chao-nui, Wang De-an, Nucl. Phys. A **496**, 729 (1989).
25. Huang Chao-nui, Wang De-an, Ma Wei-hsing Nucl. Phys. A **518**, 717 (1990).
26. M. Lacombe *et al.*, Phys. Rev. C **65**, 034004 (2002); A.M. Mosallem, V.V. Uzhinski, arXiv:nucl-th/0205039; arXiv:nucl-th/0208034.
27. I. Ahmad, M.A. Alvi, Phys. Rev. C **48**, 3126 (1993).
28. Ruan Wenying, Liu Youyan, J. Phys. G **21**, 537 (1995).